Journal of Marine Science and Technology

Volume 23 | Issue 4 Article 9

IMPROVING DETECTION TECHNIQUE FOR FLIGHT RECORDERS OF THE DISTRESS AIRPLANES CRASHED INTO OCEAN BY INTEGRATING INERTIAL NAVIGATION SYSTEM INTO UNDERWATER LOCATOR BEACON

Sheng-Shih Wang
Department of Electrical Engineering, National Taiwan Ocean University, Keelung, Taiwan

Hsien-Sen Hung
Department of Electrical Engineering, National Taiwan Ocean University, Keelung, Taiwan

Jyh-Jier Ho
Department of Electrical Engineering, National Taiwan Ocean University, Keelung, Taiwan, jackho@mail.ntou.edu.tw

Jie-Xian Lin
Department of Electrical Engineering, National Taiwan Ocean University, Keelung, Taiwan

Chi-Hsiao Yeh
Department of Surgery, Chang Gung Memorial Hospital, Keelung, Taiwan

IMPROVING DETECTION TECHNIQUE FOR FLIGHT RECORDERS OF THE DISTRESS AIRPLANES CRASHED INTO OCEAN BY INTEGRATING INERTIAL NAVIGATION SYSTEM INTO UNDERWATER LOCATOR BEACON

Acknowledgements

The authors acknowledge assistance and partial financial support from the Ministry of Science and Technology (NSC102-2221-E-019-040-MY3), and Chang Gung Memorial Hospital (CMRPG 2B0511, CMRPG 2B0521, CMRPG 2B0531, and CMRPG 2B0541) of Taiwan. In addition, Mr. Sheng-Shih Wang appreciates the support of China University of Science and Technology, Taiwan.

Journal of Marine Science and Technology, Vol. 23, No. 4, pp. 467-474 (2015)
DOI: 10.6119/JMST-014-1027-1

IMPROVING DETECTION TECHNIQUE FOR FLIGHT RECORDERS OF THE DISTRESS AIRPLANES CRASHED INTO OCEAN BY INTEGRATING INERTIAL NAVIGATION SYSTEM INTO UNDERWATER LOCATOR BEACON

Sheng-Shih Wang[1], Hsien-Sen Hung[1], Jyh-Jier Ho[1], Jie-Xian Lin[1], and Chi-Hsiao Yeh[2]

Key words: flight recorders, underwater locator beacon, search and recovery operations, inertial navigation system.

ABSTRACT

Flight recorder, used to analyze distress reasons, is equipped with underwater locator beacon (ULB) for being detected and recovered easily in sea. According to the recovery report for the Air France flight no. AF447 distress airplane, it nearly took two years and cost 40 million US dollars to search and recover the flight recorders. Apparently, future aviation safety could be greatly improved if earlier recovery of the flight recorders would reveal the crash reasons sooner. Therefore, this paper is aimed to develop an enhanced ULB, which integrates inexpensive inertial navigation system (INS) into ULB, for a cost-effective and time-saving operation of search and recovery in the future. This new equipment is anticipated to directly provide the location of flight recorders to the search and recovery authority. From the static and dynamic tests, maximum position errors are below 50 m when the stand-alone INS operates in a duty cycle of 78 seconds. From the case report of AF447 aircraft crush, the time taken from 38,000 feet (= 11,582 m) descent to sea level is about 3 minutes and 30 seconds. Over this time frame, the maximum position error is about 140 m owing to the nearly linear drift property of the INS. Thus, the proposed INS-aided ULB approach should be feasible to the search and recovery mission.

Fig. 1. The flight data recorder coated in orange color, the unit circled in dash line is underwater locator beacon.

I. INTRODUCTION

When airplanes crash to the ground, searching and rescuing people on board without the aid of an emergency beacon's distress signal is like looking for a needle in the haystack. The function of distress beacon is homing for search and rescue authorities and helps in the detection and location of aircraft in distress. The emergency beacon of aircrafts used over sea level is emergency locator transmitter (ELT), while used under sea level is underwater locator beacon (ULB). When activated, the beacon of ELT or ULB is transmitted at specified frequencies.

Flight recorders, each including cockpit voice recorder (CVR) and flight data recorder (FDR), being known as "black boxes", are mandatory equipments in commercial airplanes. FDR (as shown in Fig. 1) records specific flight parameters, including the airspeed, altitude, acceleration, heading, control

Paper submitted 06/12/14; revised 10/01/14; accepted 10/27/14. Author for correspondence: Jyh-Jier Ho (e-mail: jackho@mail.ntou.edu.tw).
[1] *Department of Electrical Engineering, National Taiwan Ocean University, Keelung, Taiwan, R.O.C.*
[2] *Department of Surgery, Chang Gung Memorial Hospital, Keelung, Taiwan, R.O.C.*

and actuator positions, engine operation and time, etc. CVR records conversations in the cockpit, radio communications between the cockpit crew and others (including air traffic control personnel), as well as ambient sounds. Each flight recorder continuously records information up to 25 hours for FDR (Boeing Company, 1998) and 2 hours for CVR (Tooley and Wyatt, 2009), and can be immensely helpful to determine the causes of a crash. With the causes the aviation industry identifies trends and makes necessary modifications to prevent future accidents.

Each flight recorder is equipped with ULB for the purpose of being detected and recovered easily in sea. The ULB is a water-activated underwater locating device, which can operate immersed to a depth of up to 20,000 feet (= 6096 m) (Kelland, 2009) and can endure active for at least 30 days once it is triggered. The ULB continuously emits an ultrasonic "pinging" pulse of 37.5 KHz at an interval of once per second at omni-direction. That provides the search and rescue authority with a means of searching for the location of the concerned flight recorder with triangulation method which needs at least two different pinger receivers to listen to the processed audio signal. A good pinger receiver may detect the ULB signal from 4-5 km away (Kelland, 2009). The distance depends on the output power of the pinger, sensitivity of the receiver, conducting media, and environmental condition (Lee et al., 2003). Bad weather or marine meteorology condition is harmful to underwater detection. The noise which results from wind scream and underwater background seriously interferes human hearing, therefore it is very difficult to use the pinger receiver.

From 2002 to 2014, there were three miserable civil airplane disasters: (1) On May 25, 2002, a Boeing 747 plane with China Airline flight No. CI611, crashed into the Taiwan Strait near Penghu Islands, causing 225 passengers and crew members killed (Aviation Safety Council, 2003); (2) On June 1, 2009, an Airbus A330 with Air France flight No. AF447, crashed into the deep Atlantic Ocean en route from Brazil to France. All 228 passengers and crew members aboard were perished (BEA, 2012); (3) On Mar 8, 2014, a Boeing 777 plane with Malaysia Airlines flight No. MH370, in which there were 239 passengers and crew members on board, disappeared en route from Kuala Lumpur to Beijing without crash site and any survivors or debris having been discovered until now (Australian Government, 2014). The resources required for the retrieval of the wreckage and recorders of the aircraft accidents are over a long period of time and are much costly. On June 19, 2002, both CVR and FDR of CI611 were recovered within battery life period of ULB. This search and recover operations (SARO) took 24 days (Aviation Safety Council, 2003) at a cost of about 12.4 million US dollars (BEA, 2014). Both CVR and FDR of AF447 were not retrieved from the Atlantic Ocean until May 2, 2011 (BEA, 2012). This SARO nearly took two years at a cost of 40 million US dollars (BEA, 2014) (or 34.6 million Euros (Ferrante et al., 2011). The question of what exactly happened to Malaysia Airlines AF370 is still unanswered after it vanished, under search by 29 aircrafts and 14 ships (Australian Government, 2014) from 26 countries (Zabludovsky, 2014). Every nation has been bearing its own costs, and it is very difficult to estimate the total amount of resources spent so far. Australian Government will cost in the order of 60 million US dollars (Australian Government, 2014) and the US Department of Defense has spent 11.4 million US dollars by April 24, 2014 in support of search operations (Warren, 2014). This accident investigation of MH370 is strictly hampered by the absence of the flight recorders, and no conclusion of this accident has been reached.

On the basis of the investigation to AF447, France's official organization, Bureau of Enquiry and Analysis for Civil Aviation Safety (Bureau d'Enquêtes et d'Analyses pour la Sécurité de l'Aviation Civile, BEA) recommend European Aviation Safety Agency (EASA) and International Civil Aviation Organization (ICAO) (1) to extend transmission time of ULB to 90 days, (2) to equip airplanes with an additional ULB transmitting on another frequency (BEA, 2014). BEA recommends later to EASA and Federal Aviation Administration (FAA) of USA that evaluating the relevance of making mandatory the record of the air data and inertial parameters (BEA, 2012).

Our research is primarily motivated by the need to recover the flight recorder at its earliest time so that the cause of the plane crash can be analyzed and determined as soon as possible. The findings of the crashed plane not only allow the aircraft manufacturers or airlines to improve aviation safety in the future, but also ease the anxiety of victims' families. Besides, the operational resources, including costs and time of search and recover will be saved significantly. The power source of this new approach device is discussed briefly in section V.

II. PROPOSED METHOD

In this paper, we propose a new approach to locate the flight recorder of a distressed aircraft by incorporating its located information into the ULB. The Enhanced-ULB (E-ULB) is designed to replace triangulation method and to directly provide the locations of FDR and CVR to the search and recovery team for finding the recorders as soon as possible. Some positioning devices such as global positioning system (GPS) and inertial navigation system (INS) are favorable candidates for providing airplane's crash site. However, the GPS receiver has a problem of the satellite radio signals blocked in deep ocean. Therefore, a strapdown INS is selected as the positioning device which can provide position with X-, Y-, and Z- components in three dimensions (3-D). In general, a typical INS is an autonomous, jamming free, and self-contained navigation module (Titterton and Weston, 2004). INS can measure the vehicle's movement based on the Newton's laws of motion, thus it can autonomously locate the flight recorders in distress. The INS consists of three units: (1) inertial sensors unit (ISU); (2) electronic unit (EU); and (3) computer unit (CU). ISU

Table 1. Definition of symbols for navigation algorithm of INS in body frame

Body Axis	Orientation	Rotation	Acceleration	Attitude	Angular velocity
X_b	forward	roll	ax	ϕ	p
Y_b	right	pitch	ay	θ	q
Z_b	down	yaw	az	ψ	r

consists of three gyroscopes and three accelerometers mounted on an orthogonal triad base and CU contains hardware and navigation algorithm. ISU combines with EU to constitute the inertial measurement unit (IMU) which measures the acceleration and angular rate of the aircraft. From these measured data, the attitude, velocity, and position (longitude, latitude and altitude) of the aircraft in earth coordination can be derived via the subsequent navigation computations.

Accelerations, sensed by accelerometers, are integrated twice to get the positions. Likewise, angular velocities, sensed by gyroscopes, are integrated once to get attitude angles. However, when operated in stand alone mode, the INS is restricted to operate in short intervals at very high update rates, because it has time-dependent error growth (Titterton and Weston, 2004). The predominant error sources of the inertial sensors are bias, scale factors and random drift. The errors encountered in the gyroscopes have the most detrimental affect on the performance of INS, owing to these errors being reflected directly into the computed attitude which is used to compute and to cancel the effect of the gravitational acceleration on the accelerometers locally (Dissanayake et al., 2001; Ferrante et al., 2011). Owing to the inherent nature of the INS, low frequency noise and sensor bias are amplified and accumulated. Until recently, the high-cost INS has kept it from being extensively installed in civilian applications. The major driving force to make use of INS is the development of cheaper inertial sensors, generally in a silicon model (Sherry et al., 2003; Godha and Cannon, 2005). However, this cost reduction of inertial sensors has also led to a significant drop in accuracy of the INS. The strap-down INS is mounted on an airplane's platform, which builds up the body frame, known as the forward-right-down frame, while the axes of navigation are north-east-down. Therefore, coordinate transformation is an important algorithm for navigation calculation. Table 1 lists the definition of orientations and symbols for INS.

The aircraft's acceleration vector $\mathbf{a}^{\mathbf{b}}$, defined in the body frame, is sensed by the three accelerometers mounted in a set of three orthogonal axes and then transformed to $\mathbf{a}^{\mathbf{n}}$, defined in the navigation frame, by the direction cosine matrix (DCM) $\mathbf{C}_{\mathbf{b}}^{\mathbf{n}}$ (Dissanayake et al., 2001). The DCM $\mathbf{C}_{\mathbf{b}}^{\mathbf{n}}$ is a 3×3 matrix and can be calculated from the angular rate measurements provided by the gyroscopes as

$$\mathbf{a}^{\mathbf{n}} = \mathbf{C}_{\mathbf{b}}^{\mathbf{n}} \mathbf{a}^{\mathbf{b}} \tag{1}$$

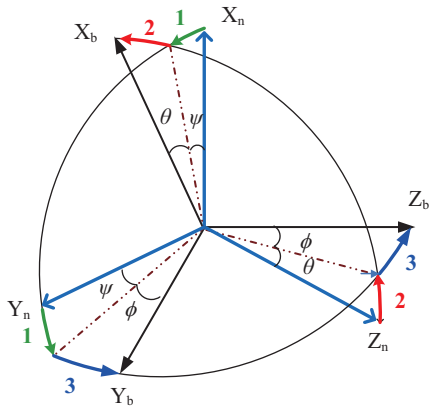

Fig. 2. The coordinate transfer between navigation frame and body frame for direction cosine matrix, where the lower case n and b represent navigation frame and body frame respectively.

$$\mathbf{C}_{\mathbf{b}}^{\mathbf{n}} = \begin{bmatrix} \cos\psi & \sin\psi & 0 \\ -\sin\psi & \cos\psi & 0 \\ 0 & 0 & 1 \end{bmatrix} \begin{bmatrix} \cos\theta & 0 & -\sin\theta \\ 0 & 1 & 0 \\ \sin\theta & 0 & \cos\theta \end{bmatrix} \begin{bmatrix} 1 & 0 & 0 \\ 0 & \cos\phi & \sin\phi \\ 0 & -\sin\phi & \cos\phi \end{bmatrix}$$

$$= \begin{bmatrix} c\theta c\psi & s\phi s\theta c\psi - c\phi s\psi & s\phi s\psi + c\phi s\theta c\psi \\ c\theta s\psi & c\phi c\psi + s\phi s\theta s\psi & c\phi s\theta s\psi - s\phi c\psi \\ -s\theta & s\phi c\theta & c\phi c\theta \end{bmatrix} \tag{2}$$

where, the letter *s* denotes *sin*, the letter *c* denotes *cos*, and the φ, θ, ψ are Euler angles of roll, pitch, and yaw in the body frame respectively. The Euler angles representing attitude are obtained by integrating the measurements from the angular velocity outputs of the three gyroscopes in X_b, Y_b, and Z_b axes. The relationship of coordinate transfer from navigation frame (X_n, Y_n, and Z_n) to body frame (X_b, Y_b, and Z_b) by direction cosine matrix is shown in Fig. 2. The coordinate transfer follows the sequence of 1-2-3 marked in Fig. 2. But the DCM takes inverse sequence for INS from body frame to navigation frame.

In inertial navigation system, the primary measurements for navigational computations are the accelerations detected by the accelerometers due to forces exerted on the airplane. For practical INS operating in the vicinity of the Earth, the output of an accelerometer triad in the navigation frame, based on the theorem of Coriolis, would be proportional to the specific force (force per unit mass) vector **f** as (Britting, 1971)

$$\mathbf{f} = \dot{\mathbf{V}}_{en} + (2\boldsymbol{\Omega}_{ie} + \boldsymbol{\Omega}_{en}) \times \mathbf{V}_{en} - \mathbf{g} \tag{3}$$

where $\mathbf{V}_{en}$ is the velocity vector in the navigation frame (platform) relative to the Earth frame (Earth-centered Earth-fixed, ECEF), $\boldsymbol{\Omega}_{ie}$ is the skew symmetric matrix form of the turn rate ω_{ie} in the Earth frame relative to the inertial frame, $\boldsymbol{\Omega}_{en}$ is the skew-symmetric matrix in the navigation frame relative to the Earth frame, and $\times$ denotes a vector cross product. In addition, $\omega_{ie} = [\mathrm{p\ q\ r}]^{\mathrm{T}}$ is the turn rate of airplane in

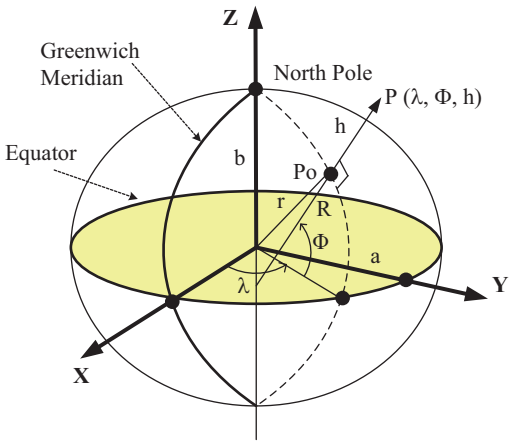

Fig. 3. Location of the airplane (position of P) is depicted by the longitude λ, geodetic latitude Φ, and altitude h in WGS-84 coordinates.

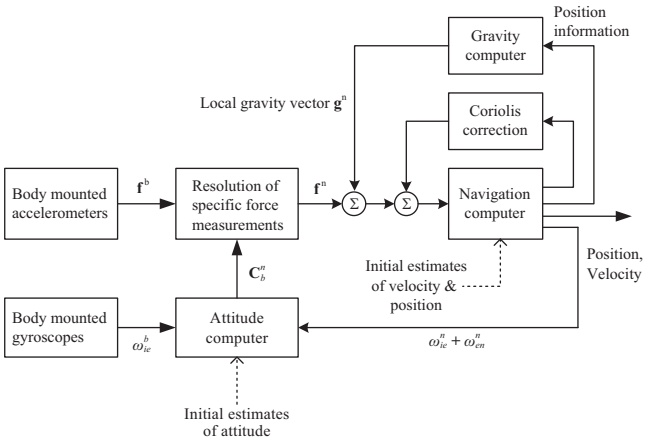

Fig. 4. A typical strapdown INS block diagram.

the Earth frame (denoted *e*) with respect to the inertial frame (denoted *i*) as measured by the gyroscopes, and **g** is the vector of gravity acceleration at the airplane location defined as

$$\mathbf{g} \equiv \mathbf{G} - \boldsymbol{\Omega}_{ie} \times \boldsymbol{\Omega}_{ie} \times \mathbf{r} \tag{4}$$

which accounts for the Earth's gravitational field **G** from the Earth center and the inward centripetal acceleration owing to the Earth's self-rotation. The **r** in (4) is the geocentric position vector in the world geodetic system 1984 (WGS-84) system, shown in Fig. 3. It should be noted that the WGS-84 system is the reference coordinate system also used in GPS. Therefore, $\mathbf{V}_{en}$ can be obtained by integration of the acceleration $\dot{\mathbf{V}}_{en}$ which can be computed from (3).

In other words, the three components of the airplane's velocity $\mathbf{V}_{en}$ along the north, east, and down directions can be obtained from

$$\mathbf{V}_{en} = \begin{bmatrix} v_n & v_e & v_d \end{bmatrix}^{\mathrm{T}} \tag{5}$$

$$v_n(t_n) = v_n(t_0) + \int_{t_0}^{t_n} a_n(t)dt$$

$$v_e(t_n) = v_e(t_0) + \int_{t_0}^{t_n} a_e(t)dt$$

$$v_d(t_n) = v_d(t_0) + \int_{t_0}^{t_n} a_d(t)dt$$

where $v(t_n)$ is the velocity at time t_n, $v(t_o)$ is the initial velocity, a is the acceleration with the subscripts n, e, and d which represent directions of north, east, and down respectively.

In the WGS-84 system, the location of airplane is depicted by the longitude (λ), latitude (Φ), and altitude (h), as shown in Fig. 3. The parameters of longitude λ, geodetic latitude Φ, and altitude h are computed in (6).

$$\left.\begin{aligned} \dot{\Phi} &= \frac{v_n}{R_M + h} \\ \dot{\lambda} &= \frac{v_e}{(R_P + h)\cos\Phi} \\ \dot{h} &= -v_d \end{aligned}\right\} \tag{6}$$

where R_M is meridian radius of curvature, R_P is transverse radius of curvature at given latitude (Grewal et al., 2007).

$$R_P = \frac{a}{(1 - e^2 \sin^2 \Phi)^{1/2}} \tag{7}$$

$$R_M = \frac{a\,(1 - e^2)}{(1 - e^2 \sin^2 \Phi)^{3/2}} \tag{8}$$

In (7) and (8), a is the semi-major axis and e is the major eccentricity of the Earth. The values of a and e can be acquired from WGS-84 system. Thus, the position of the airplane can be determined. Once v_n, v_e, and v_d are determined, the λ, Φ, and h can be obtained by integrating (6) as

$$\left.\begin{aligned} \lambda &= \lambda_0 + \int_{t_0}^{t_n} \dot{\lambda}\, dt \\ \Phi &= \Phi_0 + \int_{t_0}^{t_n} \dot{\Phi}\, dt \\ h &= h_0 + \int_{t_0}^{t_n} \dot{h}\, dt \end{aligned}\right\} \tag{9}$$

where λ_0, Φ_0, and h_0 are the initial position of aircraft respectively.

As mentioned earlier, the navigation error diverges with time causing a worse accuracy in long-term operation, especially for a low-cost INS. The drift error in position is mainly caused by bias and instability of both gyroscopes and accelerometers. Integrating calculation in CU is an error source too. A typical strapdown INS block diagram is shown in Fig. 4

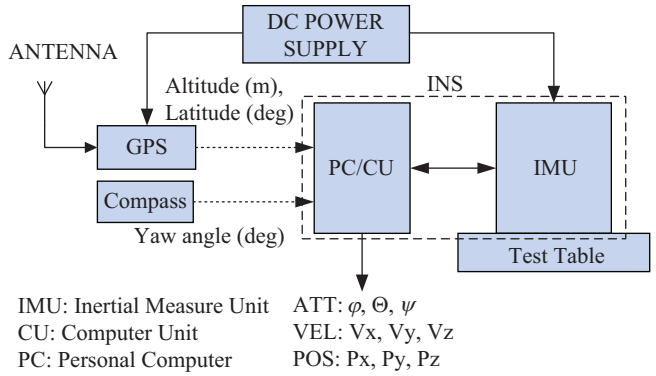

Fig. 5. Schematic structure for INS system test in which PC plays the role as CU of INS. GPS and compass provide initial data to navigation algorithm for integration. The initial data will actually come from aircraft avionics. The ATT, VEL and POS denote attitude, velocity and position of airplane respectively.

(a) (b)

Fig. 6. INS system test equipments (a) static test conducted on a horizontal rotation table, and (b) dynamic test conducted on a Scorsby motion test platform, which is derived by single shaft, rotating in a cone.

(Titterton and Weston, 2004), wherein the letter *b* represents body frame and letter *n* represents navigation frame.

III. EXPERIMENTS

In order to explore the characteristics of a low-cost INS, a system structure is set up in our laboratory, as shown in Fig. 5, in which GPS and compass are used to conduct initial alignment and to provide initial data to navigation algorithm for calculations. The initial data will actually come from aircraft avionics. The experiments for static and dynamic tests use a low-cost INS and two different platforms. The static test was carried out using a level platform at eight different yaw angles (horizontal azimuth). The dynamic test was performed using a Scorsby motion test platform which simulates aircraft's moving. Scorsby platform is derived by single shaft, rotating in a cone track, as shown in Fig. 6.

During tests, the INS runs navigation algorithm only for a duty cycle of 78 seconds, which is restricted by manufacturer. In fact, the INS always stops at original place without moving. This method enables us to measure the drift errors of X-, Y-, and Z-axis position which are represented by ΔP_X, ΔP_Y, and ΔP_Z.

Table 2. The mean and standard deviation of IMU for four Yaw angles at short term, d/s means degree per second, m/s^2 means meter per square second. Gyroscope output is shown in (a) and accelerometer output is shown in (b).

(a)

Yaw	Statistics	ω_x(d/s)	ω_y(d/s)	ω_z(d/s)
0°	mean	-0.0059	-1.5971	-1.9971
	σ	0.1403	0.0780	0.0614
90°	mean	0.1293	-1.3611	-1.8037
	σ	0.1344	0.0805	0.2025
180°	mean	0.1705	-1.2831	-1.4598
	σ	0.1597	0.0765	0.1348
270°	mean	0.1909	-1.0908	-1.3423
	σ	0.1067	0.0831	0.1286

(b)

Yaw	Statistics	a_x(m/s^2)	a_y(m/s^2)	a_z(m/s^2)
0°	mean	0.0141	0.0172	-9.8580
	σ	0.0323	0.0215	0.0268
90°	mean	-0.0475	-0.0115	-9.8722
	σ	0.0485	0.0220	0.0223
180°	mean	-0.0418	0.0526	-9.8764
	σ	0.0821	0.0280	0.0365
270°	mean	0.0210	0.0656	-9.8830
	σ	0.0871	0.0232	0.0216

IV. RESULTS AND DISCUSSIONS

1. Initial Alignment

In the step of initial alignment (leveling), initial values of navigation computation, obtained from the GPS receiver and compass, were altitude of 204.8 m, latitude of 24.72° and yaw (heading angle) of 0°. The DCM at $t = t_o$ (start time of integration) after initial alignment is shown below.

$$\mathrm{DCM}(t_0) = \begin{bmatrix} C11 & C21 & C31 \\ C12 & C22 & C32 \\ C13 & C23 & C33 \end{bmatrix}$$

$$= \begin{bmatrix} 1.0000e+00 & 0.0000e+00 & -1.6602e-03 \\ -3.3838e-06 & 1.0000e+00 & -2.0382e-03 \\ 1.6602e-03 & 2.0382e-03 & 1.0000e+00 \end{bmatrix}$$

The DCM in the strapdown INS acts as a gimbaled platform to compensate initial errors via the step of initial alignment.

2. Static Test

After initial alignment, the INS was started to run the navigation algorithm for a duty cycle of 78 seconds, and the measurements from the IMU were taken thereafter. By changing the azimuth angle from initial yaw angle at an increment of 45° each time, the aforementioned procedures were

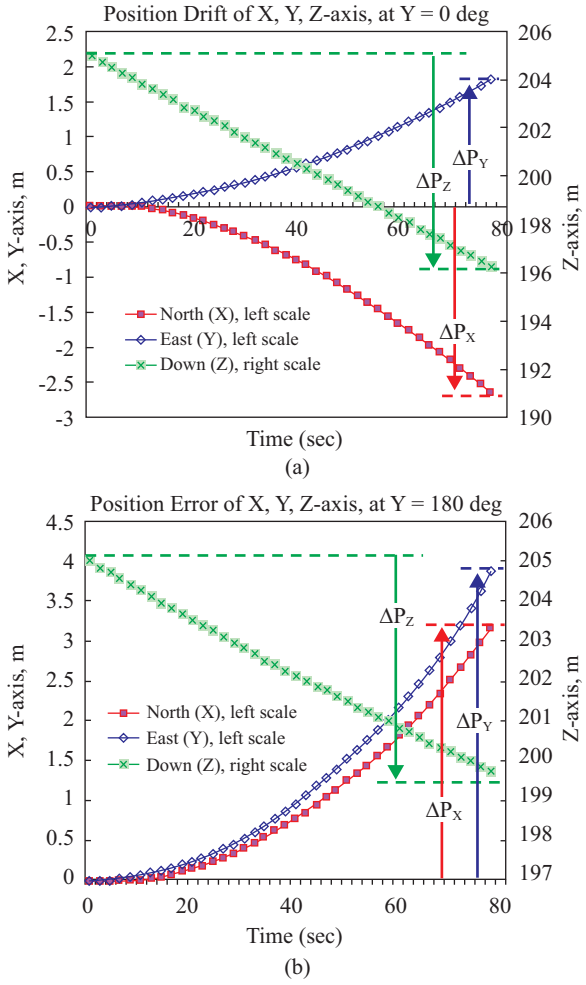

Fig. 7. Position drifts in X-, Y- , and Z-axis of INS for static test at (a) Yaw = 0° and (b) Yaw = 180°. Other position drifts at Yaw = 45°, 90°, 135°, 225°, 270° and 315° are similar and can be omitted. Symbols of ΔP_X, ΔP_Y, and ΔP_Z represent position errors due to INS drift and other errors.

repeated and measurements were taken for a total of eight different yaw angles ranging from 0° to 315°.

The mean and standard deviation were computed in statistics of gyroscopes in ω (degree/sec) and accelerometers in *a* (m/sec^2) at yaw angles of 0°, 90°, 180°, and 270° as presented in Table 2. Wherein 15 randomly selected data from the IMU at each yaw angle were measured. The short-term errors, expressed in terms of the standard deviation σ, are not significant except that the σ of x-axis gyroscope is larger than those of the other axes by one order-of-magnitude (10^1).

The X-, Y-, and Z-axis position drifts of the INS at yaw angles of 0° and 180° are shown in Fig. 7(a) and (b) respectively. These figures, which depict the position drift as a function of time, are collected from PC. These results show that position errors diverge as time evolves. The position errors of INS at eight different yaw angles for static test are summarized in Table 3, from which we observe that the maximum position errors in X-, Y-, and Z-axis are 7 m, 3.8 m and 36.8 m respectively. Two significantly larger position errors appear at Z-axis when the yaw angles are 225° and 315°. The maximum static position error is 36.8 m in Z-axis at the yaw angle of 315° after performing Navigation Mode for an interval of 78 seconds.

Table 3. The INS position error for three components in static test at eight different yaw angles, the unit is meter.

Axis	Position error (m) at Yaw angles							
	0°	45°	90°	135°	180°	225°	270°	315°
X	-2.7	-7.0	2.7	0.7	3.2	-4.0	-1.0	0.8
Y	1.8	-0.1	2.8	-0.3	3.8	0.02	-0.2	-1.9
Z	8.3	8.3	2.0	1.8	5.1	35.8	1.3	36.8

From Fig. 7 and Table 3, we can observe that there is no regularity for the position error variation of the same position parameter ΔP_X and ΔP_Y, except for ΔP_Z. One possible reason for ΔP_Z drifting nearly linear may be that earth self-rotation rate sensed by gyroscope of Z-axis is not cancelled in the navigation loop.

3. Dynamic Test

Contrast to the static tests wherein the table is placed horizontally changing yaw angels each time, the dynamic test of the INS was performed using the Scorsby motion test table which simulates the roll, pitch, and yaw motions of an aircraft during flight. Schematic structure for INS system dynamic test is shown in Fig. 6(b). The three-axis outputs of INS in attitude and position in counterclockwise is shown in Fig. 8. From Fig. 8(a), the sinusoidal period is about 10 sec, which is equal to the motion table's turning rate. As for yaw angel, there is a divergence of 6.66° at 78th sec. Fig. 8(b) shows the three position components of INS. For the same experiment period, the position drifts for X-, Y-, and Z-axis are less than 19 m. The initial position of Z-axis is 204.8 m over mean sea level (MSL), but 133 m shown in the plot.

Fig. 9 shows the three-axis outputs of INS in attitude and position in clockwise. Fig. 9(b) shows the three position components of INS. For the same experiment period, the position difference for X-, Y-, and Z-axis are less than 30 m, 28 m, and 50 m respectively. The initial position of Z-axis is 204.8 m over mean sea level (MSL), but 120 m shown in the plot. According to the plots shown in Fig. 8(b) and 9(b), the Z-axis signal malfunctions. This can be verified from the divergent behavior in the sinusoidal curves of yaw in Fig. 8(a) and 9(a).

Since the position drift results are similar to those of the static test, only the position errors of the dynamic test are summarized in Table 4. The maximum position errors in X-axis, Y-axis and Z-axis are 30 m, 28 m and 50 m, respectively, when the Scorsby motion table rotates in clockwise direction after performing navigation for an interval of 78 seconds. The position error of 50 m in Z-axis may be caused by thermal accumulation of motor in gyroscope and of torquer in accelerometer, which makes performance worse.

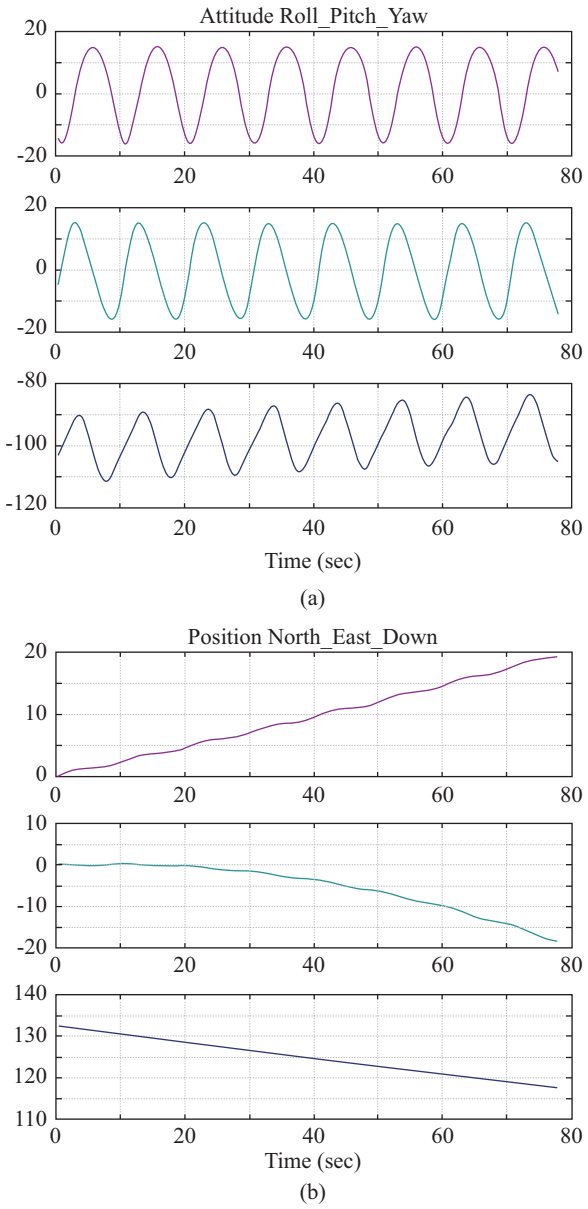

Fig. 8. Three-axis outputs of INS for (a) attitude in degree, (b) position in m. Scorsby motion table rotates counterclockwise.

The INS has drift characteristic that can cause position errors to grow with time. The main reasons for the increase of position error are attributed to IMU sensors' errors, including bias, scale factor, non-orthogonality, gyroscopes drift (due to temperature changes), and random noise (Grejner-Brzezinska and Wang, 1998). When gyroscopes and accelerometers continually run, they will produce heat owing to current flowing coils, thus in turn deteriorating the performance of INS.

Since gyroscopes and accelerometers drift with time, real-time aircraft's position must be updated regularly with the aid of GPS. A commercialized INS, specially used for recorders of airplanes, is better to have features of low-cost, robustness and compact. On the other hand, any INS before serving on board must be tested completely. There are two kinds of test for INS, namely, function test and environment stress test. The function test includes static test, dynamic test (both carried out in this paper), and long-term test. The environment stress test includes temperature, vibration, shock, water-proof to check if INS can endure in worst mission environment. Those tests will be undertaken in the future.

Table 4. The position error of INS at dynamic test.

Axis	Position error	
	Counterclockwise	Clockwise
X	19 m	30 m
Y	19 m	28 m
Z	15 m	50 m

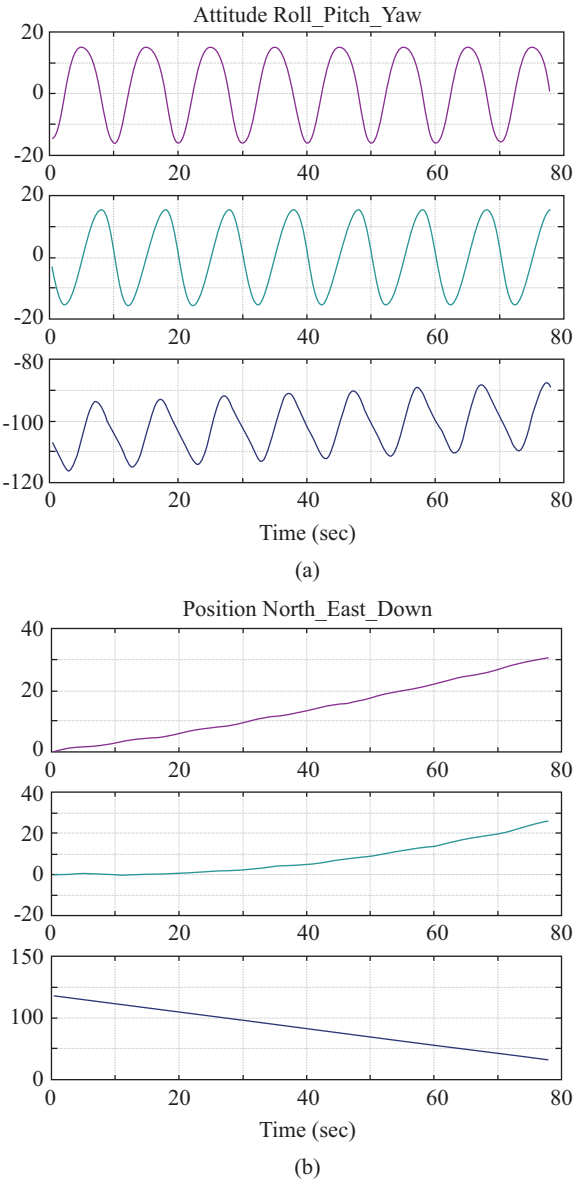

Fig. 9. The three-axis outputs of INS for (a) attitude in degree, (b) position in m. Scorsby motion table rotates clockwise.

V. CONCLUSION AND FUTURE PERSPECTIVE

The objective of this research is to improve technique of detection and location for flight recorders of the distress airplanes crashed into ocean, and then to provide a more refined fix on crash location. This can be achieved by a new approach in this paper that integrated INS with ULB to decrease SARO period and cost. From the static and dynamic tests, maximum position errors are about 50 m when the stand-alone INS operates in a duty cycle of 78 seconds. According to the experience of AF447, the time taken from level of 38,000 feet (= 11,582 m) descent to sea level is about 3 minutes and 30 seconds (Shaikh, 2011). Over this time frame, the maximum position error is about 140 m owing to the nearly linear drift property of the INS. Thus, the proposed INS-aided ULB should be feasible to the search and recovery mission.

Of particular importance is that the inertial sensors based on micro-electro-mechanical system technology are small, cheap and robust, but exhibit less accuracy. In order to improve accuracy, the navigation data can be processed through signal estimation theory. Since INS is a nonlinear model, extended Kalman filter or particle filter is more suitable for the estimation of a nonlinear system (Gustafsson et al., 2002). To establish an INS error model, the state vector containing the sensor errors like bias, scale factor error and gyroscope constant drift rate must be taken into account. The hybrid system may have potentially significant advantages of miniaturization in size as well as reduced cost, weight, and power consumption. The extra electrical power can be used to enhance transmit power to extend detectable range. The E-ULB will be more sophisticated than the traditional ULB if an unique identification code of airplane is to be installed in CU. In contrast to enormous efforts of time and money having been made in recovering flight recorders of CI611, AF447 and MH370, the cost that E-ULB needs to pay is apparently worthwhile.

Because a crashed airplane will not provide electric power any longer. The solar cells can be employed to provide electric power to prolong operation period of the new approach system (INS-aided ULB) by charging the battery. Therefore open circuit voltage (V_{OC}) of solar cells is more important than short current density (J_{SC}), conversion efficiency (η). It is necessary to select a suitable material and structure of solar cells.

ACKNOWLEDGMENTS

The authors acknowledge assistance and partial financial support from the Ministry of Science and Technology (NSC102-2221-E-019-040-MY3), and Chang Gung Memorial Hospital (CMRPG 2B0511, CMRPG 2B0521, CMRPG 2B0531, and CMRPG 2B0541) of Taiwan. In addition, Mr. Sheng-Shih Wang appreciates the support of China University of Science and Technology, Taiwan.

REFERENCES

Australian Government (2014). Joint Agency Coordination Centre MH370 Transcript of Press Conference. retrieved April 28, 2014 from http://www.jacc.gov.au/media/interviews/2014/april/tr011.aspx

Aviation Safety Council (2003). CI611 Accident Investigation Factual Data Report. ASC-AFR-03-06-001, Taipei, Taiwan, ROC.

BEA (Bureau of Enquiry and Analysis for Civil Aviation Safety) (2012). On the accident on 1st. June 2009 to the Airbus A330-203 registered F-GZCP operated by Air France flight AF 447 Rio de Janeiro – Paris.

BEA (Bureau of Enquiry and Analysis for Civil Aviation Safety) (2014). Flight Data Recovery Working Group Report. Retrieved March 12, 2014 from http://www.bea.aero/en/enquetes/flight.af.447/flight.data.recovery.working.group.final.report.pdf

Boeing Company (1998). Flight Data Recorder Rule Change. Aero Magazine 02, Spring. Retrieved March 20, 2014 from http://www.boeing.com/commercial/aeromagazine/aero_02/textonly/s01txt.html

Britting, K. R. (1971). Inertial Navigation System Analysis, Willy, New York.

Dissanayake, G., S. Sukkarieh, E. Nebot and H. Durrant-Whyte (2001). The aiding of a low-cost strapdown inertial measurement unit using vehicle model constraints for land vehicle applications. IEEE Transactions on Robotics and Automation 17, 731-747.

Ferrante, O., M. Kutzleb and M. Purcell (2011). AF447 Underwater Search and Recovery Operations A Shared Government-Industry Process. International Society of Air Safety Investigators (ISASI) Forum Oct-Dec, 18-25.

Godha, S. and M. E. Cannon (2005). Integration of DGPS with a Low Cost MEMS–Based Inertial Measurement Unit for Land Vehicle Navigation Application. Proceedings of International Technical Meeting of the Satellite Division of The Institute of Navigation (ION GNSS 2005), Long Beach, CA, 333-345.

Grejner-Brzezinska, D. A. and J. Wang (1998). Gravity modelling for high - accuracy GPS/INS integration. Navigation 45, 209-220.

Grewal, M. S., L. R. Weill and A. P. Andrews (2007). Global Positioning Systems, Inertial Navigation, and Integration. Willy, New Jersey, USA.

Gustafsson, F., F. Gunnarsson, N. Bergman, U. Forssell, J. Jansson, R. Karlsson and P.-J. Nordlund (2002). Particle filters for positioning, navigation, and tracking. IEEE Transactions on Signal Processing 50, 425-437.

Kelland, N. C. (2009). Deep-water Black Box Retrieval. Hydro International. Retrieved Jan. 22, 2014 from http://www.hydro-international.com/issues/articles/id1130-Deepwater_Black_Box_Retrieval.html

Lee, D., S. Su and K. Yong (2003). CI611 and GE791 Wreckage Recovery Operations-Comparisons and Lessons learned. Proceedings of Annual International Seminar of International Society of Air Safety Investigators (ISASI), Washington, D.C., USA, 38-42.

Shaikh, T. (2011). Air France crash pilots lost vital speed data, says investigators. CNN, May 27, Retrieved May 28, 2013 from http://www.cnn.com/2011/WORLD/americas/05/27/air.france.447.crash/index.html

Sherry, L., C. Brown, B. Motazed and D. Vos (2003). Performance of automotive grade MEMS sensors in low cost AHRS for general aviation. IEEE Digital Avionics Systems Conference, IN, USA,12.c.2-1-12.c.2-4.

Titterton, D. H. and J. L. Weston (2004). Strapdown inertial navigation technology. 2nd Ed., The Institution of Electrical Engineers, UK. and The American Institute of Aeronautics and Astronautics, VA. USA.

Tooley, M. and D. Wyatt (2009). Aircraft Electrical and Electronic Systems. Butterworth-Heinemann, Oxford, UK.

Warren, S. (2014). News Article: Maintains Support to Find Missing Malaysia Airlines Flight 370. American Forces Press Service, Retrieved April 24, from http://www.defense.gov/news/newsarticle.aspx?id=122122

Zabludovsky, K. (2014). Costs Soaring, Air Search for MA370 Ends, but Undersea Mission Continues. Newsweek, Retrieved April 28, from http://www.newsweek.com/costs-soaring-air-search-malaysia-airlines-flight-370-ends-undersea-mission-248869.